Superconductivity induced by doping platinum in BaFe$_2$As$_2$

Xiyu Zhu,[1] Fei Han,[1] Gang Mu,[1] Peng Cheng,[1] Jun Tang,[2] Jing Ju,[2] Katsumi Tanigaki,[2] and Hai-Hu Wen[1,*]

[1]*National Laboratory for Superconductivity, Institute of Physics and Beijing National Laboratory for Condensed Matter Physics, Chinese Academy of Sciences, P.O. Box 603, Beijing 100190, China*

[2]*World Premier International Research Center, Tohoku University, Sendai 980-8578, Japan*

By substituting Fe with the 5d-transition metal Pt in BaFe$_2$As$_2$, we have successfully synthesized the superconductors BaFe$_{2-x}$Pt$_x$As$_2$. The systematic evolution of the lattice constants indicates that the Fe ions were successfully replaced by Pt ions. By increasing the doping content of Pt, the antiferromagnetic order and structural transition of the parent phase is suppressed and superconductivity emerges at a doping level of about $x=0.02$. At a doping level of $x=0.1$, we get a maximum transition temperature T_c of about 25 K. While even for this optimally doped sample, the residual resistivity ratio is only about 1.35, indicating a strong impurity scattering effect. We thus argue that the doping to the Fe sites naturally leads to a high level impurity scattering, although the superconductivity can still survive at about 25 K. The synchrotron powder x-ray diffraction shows that the resistivity anomaly is in good agreement with the structural transition. The superconducting transitions at different magnetic fields were also measured at the doping level of about $x=0.1$, yielding a slope of $-dH_{c2}/dT=5.4$ T/K near T_c. Finally a phase diagram was established for the Pt-doped 122 system. Our results suggest that superconductivity can also be easily induced in the FeAs family by substituting the Fe with Pt with almost the similar maximum transition temperatures as doping Ni, Co, Rh, and Ir.

PACS number(s): 74.70.Dd, 75.30.Fv, 74.10.+v

I. INTRODUCTION

The FeAs-based compounds have formed a new family in the field of high-T_c superconductors.[1] Many new structures with the FeAs layers have been found, including the so-called 1111 phase (LNFeAsO, AEFeAsF, LN=rare-earth elements, AE=alkaline-earth elements),[1–3] 122 phase (AEFe$_2$As$_2$, AE=alkaline-earth elements),[4,5] 111 phase (LiFeAs, NaFeAs),[6,7] 11 phase (FeSe),[8] 32522 phase (Sr$_3$Sc$_2$O$_5$Fe$_2$As$_2$),[9] and 21311 phase (Sr$_2$ScO$_3$FeP and Sr$_2$VO$_3$FeAs).[10,11] In the system of (Ba,Sr)$_{1-x}$K$_x$Fe$_2$As$_2$ with the ThCr$_2$Si$_2$ structure (denoted as 122 phase), the maximum T_c at about 38 K was discovered[4,5] at about $x=0.40$. Large single crystals can be grown in this 122 system.[12,13] It has been already found that by substituting the Fe sites with the 3d, 4d, and 5d transition metals such as Co,[12,14,15] Ni,[16] Ru,[17] Rh, Pd, and Ir,[18,19] the superconductivity can be induced. It is thus necessary to see whether doping another 5d element Pt can also induce superconductivity in the 122 phase. In this paper, we report the successful fabrication of the new superconductor BaFe$_{2-x}$Pt$_x$As$_2$ with the maximum T_c of about 25 K at the doping level of $x=0.1$. X-ray diffraction (XRD) pattern, resistivity, synchrotron powder x-ray diffraction, dc magnetic susceptibility and upper critical field have been measured in this Pt-doped system. We also explored the phase diagram concerning the gradual vanishing of the antiferromagnetic (AF) order and the establishment of superconductivity upon doping Pt in this system.

II. SAMPLE PREPARATION

The polycrystalline samples BaFe$_{2-x}$Pt$_x$As$_2$ were synthesized by using a two-step solid-state reaction method. First, BaAs, PtAs, and Fe$_2$As powders were obtained by the chemical reaction with Ba pieces, Pt powders (purity 99.95%), Fe powders (purity 99.99%) and As grains. Then they were mixed together in the formula BaFe$_{2-x}$Pt$_x$As$_2$, ground and pressed into a pellet shape. All the weighing, mixing, and pressing procedures were performed in a glove box with a protective argon atmosphere (both H$_2$O and O$_2$ are limited below 0.1 ppm). The pellet was sealed in a silica tube with 0.2 bar of Ar gas and followed by a heat treatment at 900 °C for 30 h. Then it was cooled down slowly to room temperature.

III. EXPERIMENTAL DATA AND DISCUSSION

The x-ray diffraction measurements were performed at room temperature using an MXP18A-HF-type diffractometer with Cu $K\alpha$ radiation from 10° to 80° with a step of 0.01°. Synchrotron powder XRD experiments were performed on a large Debye-Scherrer camera installed at SPring-8 beam line BL02B2 by using an imaging plate as the detector. The wavelength of the x ray was determined to be 0.602 Å by using CeO$_2$ as the reference. Glass capillaries with an inner diameter of 0.3 mm were used to hold the powder samples in order to eliminate the preferred orientation. The Rietveld refinements were carried out using GSAS in the angle range of 2° to 75° with an increment of 0.01°.[20] The dc magnetization measurements were done with a superconducting quantum interference device (Quantum Design, SQUID, MPMS7). The zero-field-cooled (ZFC) magnetization was measured by cooling the sample at zero field to 2 K, then a magnetic field was applied and the data were collected during the warming up process. The field-cooled magnetization data has been collected in the warming up process after the sample was cooled down to 2 K at a finite magnetic field. The resistivity measurements were done with a physical property measurement system PPMS-9T (Quantum Design) with the four-probe technique. The current direction was reversed for mea-
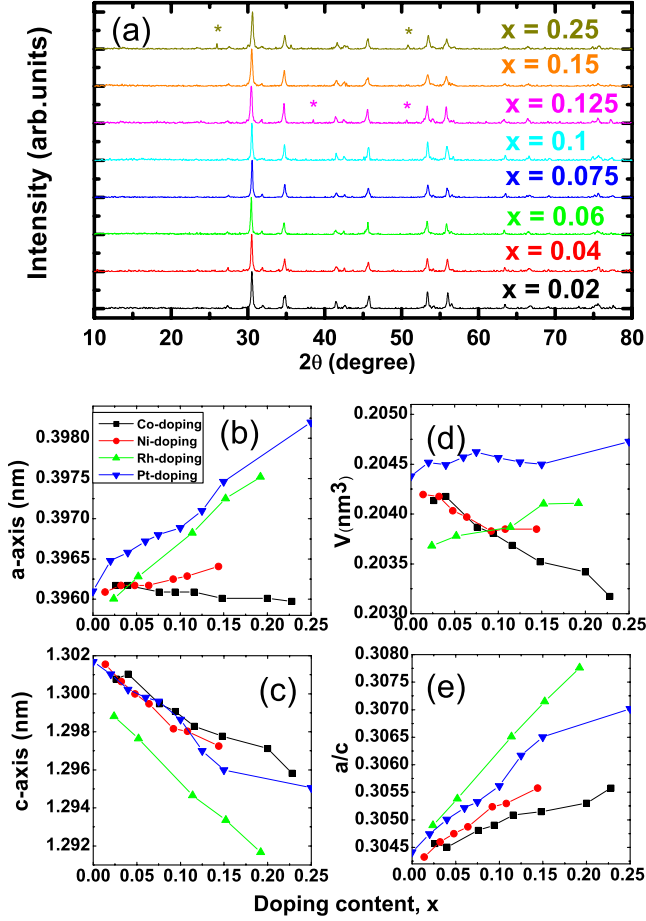
FIG. 1. (Color online) (a) X-ray diffraction patterns of the samples $BaFe_{2-x}Pt_xAs_2$. Almost all main peaks can be indexed to the tetragonal structure yielding the values of lattice constants. The asterisks mark the peaks arising from the impurity phase $PtAs_2$. [(b) and (c)] Doping dependence of the a-axis lattice constant and c-axis lattice constant of the Co, Ni, Rh, and Pt doping. Here we use the same notation of the doping content x in $BaFe_{2-x}TM_xAs_2$ (TM =Co, Ni, Rh, and Pt). It is clear that the a-axis lattice constant expands while the c-axis one shrinks monotonically with transition-metal substitution. This systematic evolution clearly indicates that the Pt ions have been successfully substituted into the Fe sites. [(d) and (e)] Doping dependence of the unit-cell volume and the ratio a/c versus doping content x in $BaFe_{2-x}TM_xAs_2$ (TM =Co, Ni, Rh, and Pt). The data of Rh and Pt doping are extracted from our experiments while those for Ni and Co doping are from the paper of Canfield (Ref. 22).

suring each point in order to remove the contacting thermal power.

A. X-ray diffraction

In order to have a comprehensive understanding to the evolution induced by the doping effect, we have measured the x-ray diffraction patterns for $BaFe_{2-x}Pt_xAs_2$ with x from 0 to 0.25. The lattice constants along a axis and c axis are thus obtained. In Fig. 1(a), we present the x-ray diffraction patterns of $BaFe_{2-x}Pt_xAs_2$. It is clear that all main peaks of the samples can be indexed to the $ThCr_2Si_2$ structure. The
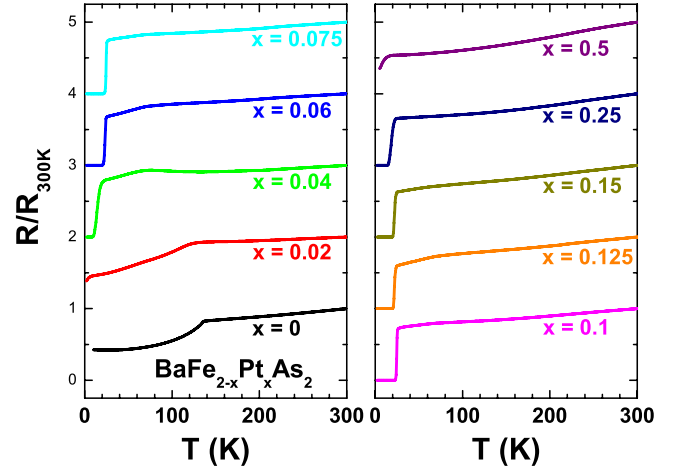

FIG. 2. (Color online) Temperature dependence of resistivity for samples $BaFe_{2-x}Pt_xAs_2$ with x ranging from 0 to 0.5. The superconductivity starts to appear at $x=0.02$, reaching a maximum T_c of 25 K at about $x=0.1$.

peaks marked with asterisks arise from the impurity phase $PtAs_2$. As we can see, only the samples with high doping levels have the impurity phase $PtAs_2$. By fitting the XRD data to the structure with the software POWDER-X,[21] we get the lattice constants of $BaFe_{2-x}Pt_xAs_2$. In Figs. 1(b) and 1(c), we show a- and c-axes lattice parameters for the $BaFe_{2-x}Pt_xAs_2$ samples. One can see that, by substituting Pt into Fe sites, the lattice constant a expands, while c shrinks. This tendency is similar to the case of doping the Fe sites with Ni, Rh, Ir, or Ru.[17–19] For Ni and Co doping, the variation in a-axis lattice constant seems weaker, but the c-axis lattice constant drops significantly. Normally a larger a-axis and smaller c-axis lattice constant would mean that the bond angle of As-Fe-As is getting larger. Therefore the parameter $(a/c)/(a_0/c_0)$ (a_0 and c_0 are the lattice constants for the parent phase) should tell us some information the doping induced change in bond angle and superconductivity. In Figs. 1(d) and 1(e) we present the doping dependence of the unit-cell volume and the ratio a/c versus doping content x. Here we compared $(a/c)/(a_0/c_0)$ with other dopants in Fig. 1(e).[19,22] The optimal doping for Pt was found at about 0.1, with $(a/c)/(a_0/c_0)$ of about 1.005, while it is also near 1.005 for Rh and Pd-doped samples at optimal doping.[19] However $(a/c)/(a_0/c_0)$ for Co- and Ni-doped samples at optimal doping is much smaller than Pt-doped samples.[22] Regarding the relatively similar T_c values in all these systems, it is tempting to conclude that the value of $(a/c)/(a_0/c_0)$ is not a decisive parameter to govern the superconductivity.

B. Doping dependence of resistivity

In Fig. 2, we show the temperature dependence of resistivity for $BaFe_{2-x}Pt_xAs_2$ samples under zero field in the temperature region up to 300 K. The resistivity anomaly T_{an} is determined as the point deviating from the linear part at high temperatures. As we can see, the parent phase $BaFe_2As_2$ exhibits a sharp drop of resistivity (resistivity anomaly) at about 140 K, which associates with the formation of the
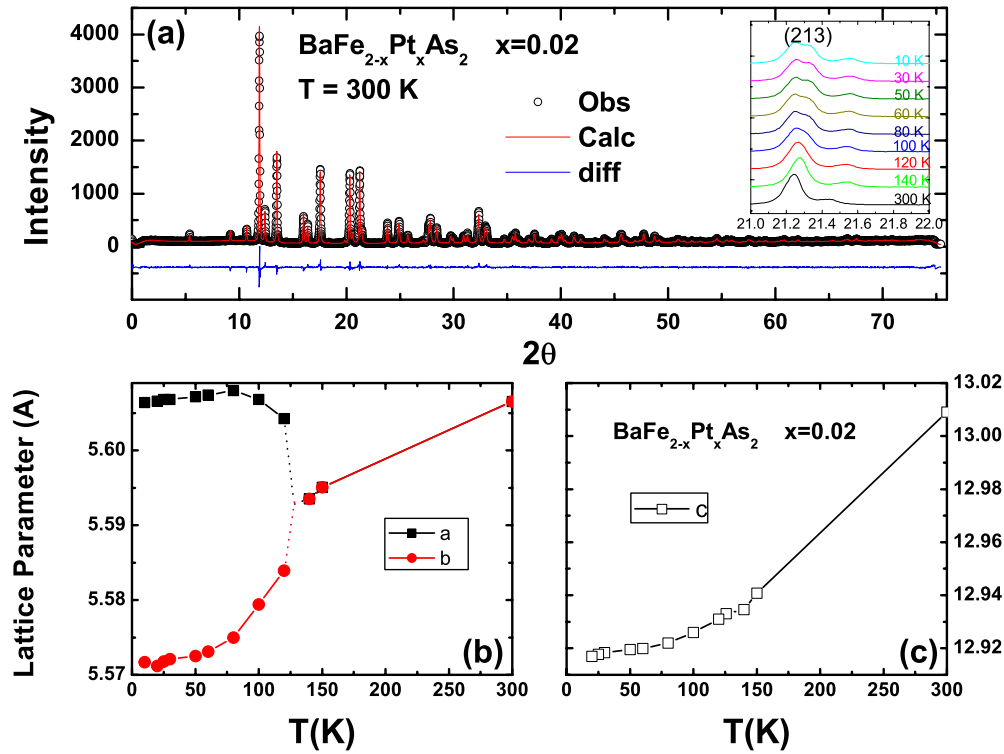
FIG. 3. (Color online) Synchrotron powder x-ray diffraction and the Rietveld fit for $BaFe_{1.98}Pt_{0.02}As_2$. The lattice parameters shrink with the decreasing of temperature. At about 125 K, the tetragonal-orthorhombic structural phase transition occurs, this can be easily seen in the inset shown for the peak (213).

antiferromagnetic order and structural transition. By doping more Pt, the resistivity drop was converted to an uprising. We found that the superconductivity appears in the sample with nominal composition of $x=0.02$, which may be induced by a small amount of superconducting phase, suggesting slight inhomogeneity in the sample. At this doping level, the resistivity anomaly T_{an} is about 128 K, being rather consistent with the structure transition temperature (as shown in Fig. 3). As the doping level was raised to 0.04, the resistivity anomaly T_{an} moves to 108 K, which is also consistent with the structure transition temperature. In the sample with $x=0.1$, we get a maximum transition temperature T_c of about 25 K, which is determined by a standard method, i.e., using the crossing point of the normal-state background and the extrapolation of the transition part with the most steep slope (as shown by the dashed lines in Fig. 5). The transition width determined here with the criterion of $10-90\%$ ρ_n (ρ_n means the normal-state resistivity at the onset transition point) is about 1.87 K. According to Saha *et al.*,[23] the superconducting transition temperature T_c on the single crystal with $x=0.1$ is about 23 K while the transition width is about 1.5 K. Comparing with our data on the polycrystalline sample with $x=0.1$, the superconducting transition temperature T_c of our sample is a little higher than theirs, which may be caused by the slight difference of the doping level. Meanwhile, the superconducting resistive transition width in our samples is a little bigger than theirs, which may be caused by the grain boundaries of polycrystalline samples. However, our data on the polycrystalline sample in regard to the superconducting transition behavior is very close to the data on the single-crystal sample.

As mentioned above, there is an impurity phase $PtAs_2$ in some samples, so it is necessary to discuss how the impurity phase might affect the resistive properties of the material. According to the x-ray diffraction data, in the low-doped samples, there is no impurity phase $PtAs_2$, therefore here we discuss only the highly doped samples. In these samples, the impurity scattering caused by $PtAs_2$ may lead to the increase in impurity scattering rate. However, as we argue below, the sizable impurity-scattering effect in these samples are not induced by the slight amount of $PtAs_2$, but by the intrinsic impurity-scattering induced by the dopants at the Fe sites. In Fig. 2 we show the normalized resistance data. Here, we take the sample $BaFe_{1.9}Pt_{0.1}As_2$ as an example to illustrate our point. For this sample, the residual resistance ratio, RRR [$\equiv\rho(300\ K)/\rho(30\ K)$] is about 1.35. This value is very small manifesting a bad metallic behavior and a strong impurity scattering. However, as evidenced by the x-ray diffraction data, our sample in this doping is quite clean, which would not lead to such a strong impurity scattering. Actually, even in the single-crystal samples with the doping to the Fe sites, RRR is also quite small. For example, in the single crystals of $BaFe_{2-x}M_xAs_2$ ($M=Pt,Pd,Rh$),[19,23] RRR is just around 2. For the single crystals with Ni and Co doping,[22,24] the RRR can at most rises up to 3, which is much below the value of the $(Sr,Ba)_{1-x}K_xFe_2As_2$ which can go up to about $8-10$ in very clean samples.[13] The very large RRR value is expectable in the samples when the out-of-plane sites, here such as the Ba/Sr atoms, are doped with K. So a small RRR in the samples with doping to the Fe sites may be a common phenomenon in this system, indicating an intrinsic strong impurity-scattering effect. It is surprising that the supercon-

ductivity can still survive up to about 25 K even with such a strong impurity-scattering effect. This result challenges the theoretical predictions on the impurity pair breaking effect with the model of the $S^\pm$ pairing manner in the iron pnictide superconductors.

C. Synchrotron powder x-ray diffraction

In order to investigate the relationship between the structural phase transition and the resistivity anomaly, synchrotron powder XRD experiments with the temperature from 10 to 300 K were performed on the samples $BaFe_{1.98}Pt_{0.02}As_2$, $BaFe_{1.96}Pt_{0.04}As_2$, and $BaFe_{1.9}Pt_{0.1}As_2$. As shown in Fig. 3, the refined crystal structure of $BaFe_{1.98}Pt_{0.02}As_2$ at room temperature is in good agreement with $ThCr_2Si_2$ structure. As the temperature decreases, the lattice constants a and c shrink a bit. The inset of Fig. 3(a) shows the (213) Bragg reflection peak as a function of temperature. The splitting of that peak indicates that the sample undergoes a tetragonal to orthorhombic distortion. The space-group symmetry changes from tetragonal ($I4=mmm$) to orthorhombic ($Fmmm$) at about 125 K. As mentioned above, the resistivity anomaly T_{an} of $BaFe_{1.98}Pt_{0.02}As_2$ is about 128 K, which is very close to that determined from the synchrotron data. So the resistivity anomaly T_{an} is rather consistent with structural transition temperature at the doping level $x=0.02$. At the doping level $x=0.04$, T_{an} is about 108 K, while the structural transition occurs between 100 and 120 K (not shown here). At the doping level $x=0.1$, no structural transition was found in the synchrotron experiment at all temperatures.

D. Electronic phase diagram

Based on the measurements described above, a phase diagram of $BaFe_{2-x}Pt_xAs_2$ within the doping range of x from 0 to 0.25 was given in Fig. 4. The T_{an} was defined as the temperatures of the anomaly in resistivity and T_c was determined from the onset of superconducting resistive transition. As we can see, with increasing Pt content, the temperature of the resistivity anomaly which corresponds to the tetragonal-orthorhombic structural/antiferromagnetic transition is driven down, and the superconductivity emerges at $x=0.02$, reaching a maximum T_c of 25 K at $x=0.1$. This general phase diagram looks very similar to that with Ni and Pd doping.[15,22] Since Pt locates just below Ni and Pd in the periodic table of elements, we would conclude that the superconductivity induced by Pt doping shares the similarity as that of Ni doping.

One of the interesting point here is that, the superconductivity transition at about 23 K was observed even up to the doping level of $x=0.25$, making the superconducting phase region extremely asymmetric. This can be naturally understood as the slow degradation of the AF spin fluctuations in the overdoped region if assuming that the paring is through exchanging the AF spin fluctuations. As indicated in our previous work in the Co-doped Ba-122 single crystals,[24] the superconducting "dome" is not symmetric at all in the iron pnictide superconductors. In the underdoped region, the superconducting transition temperature ramps quickly up to the maximum value since the superconducting phase wins more
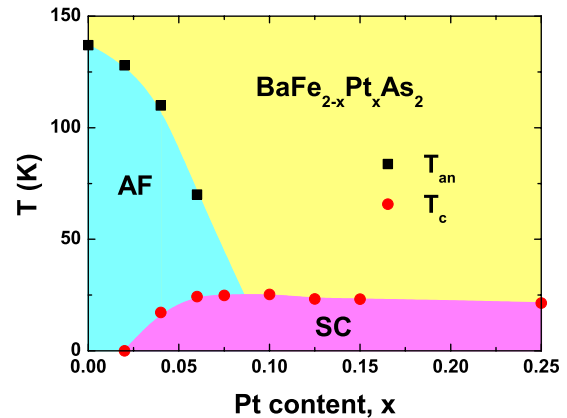

FIG. 4. (Color online) Phase diagram of $BaFe_{2-x}Pt_xAs_2$ within the doping range of $x=0-0.25$. The temperature of resistivity anomaly represents the starting point of the upturning of resistivity, i.e., the deviating point from a rough T-linear behavior in the high-temperature region. The superconductivity starts to appear at about $x=0.02$, the T_c value reaches a maximum of 25 K at $x=0.1$. The long-tail-like overdoped region may be induced by the slow degradation of the AF spin fluctuations or the percolative superconductivity.

and more density of states from the AF order. It is these quasiparticles that pair via exchanging the residual AF spin fluctuation and form the superconducting condensate. While, in the overdoped region, the whole Fermi surfaces will involve in the superconducting pairing, but now the pairing strength which is governed by the AF spin fluctuation becomes weaker and weaker. The extended superconducting transition at such a high doping level may also be partly attributed to the percolative superconductivity. The doping may have an upper solubility limit. Above this doping level, the system will chemically phase separate into two different regions, one with superconductivity at almost the optimized T_c, while the others are the impurity phases, such as $PtAs_2$. Further experiments on single crystals may decide whether this long-tail-like overdoped region is an intrinsic feature for the Pt-doped samples.

E. Upper critical field

In Fig. 5, we present the temperature dependence of resistivity under different magnetic fields for the sample with $x=0.1$. As shown in the inset (a) of Fig. 5, just as many other iron pnictide superconductors, the diamagnetic signal is very strong. However, from the zero-field-cooling $M(T)$ curve one can also see that the low-temperature part is not flat. This strong temperature dependence was not seen in the field-cooling $M(T)$ data. We explain this strong temperature-dependent ZFC $M(T)$ curve as due to the decaying of the Meissner screening current, which is induced by the easy motion the of magnetic flux (even not the superconducting quantized flux lines) through the weak links at the grain boundaries. This happens quite often in the polycrystalline samples. We thus used the criterion of 90% ρ_n to determine the upper critical field and show the data in the inset (b) of Fig. 5. A slope of $-dH_{c2}/dT=5.4$ T/K can be obtained here.
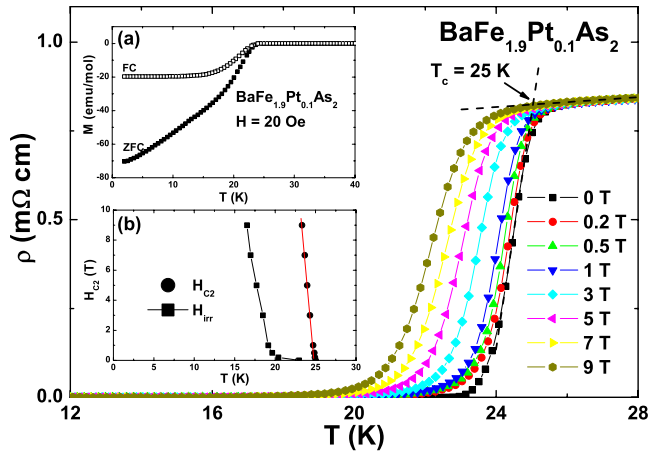
FIG. 5. (Color online) Temperature dependence of resistivity for the sample $BaFe_{1.9}Pt_{0.1}As_2$ at different magnetic fields. The dashed line indicates the extrapolated resistivity in the normal state. One can see that the superconductivity seems to be robust against the magnetic field and shifts slowly to lower temperatures. The inset (a) shows the dc susceptibility data using the zero-field-cooling and field-cooling modes with a dc magnetic field of 20 Oe. The inset (b) gives the upper critical field determined using the criterion of 90% ρ_n. A slope of $-dH_{c2}/dT = 5.4$ T/K near T_c is found here. The irreversibility line H_{irr} taking with the criterion of 0.1% ρ_n is also presented in the inset.

This is a rather large value which indicates a rather high upper critical field in this system. By using the Werthamer-Helfand-Hohenberg (WHH) formula[25] for a single band system $H_{c2}(0) = -0.69(dH_{c2}/dT)|_{T_c} T_c$, the value of zero-temperature upper critical field can be estimated. Taking $T_c = 25$ K, we can get $H_{c2}(0) \approx 93$ T roughly. This is a very large upper critical field, just as in K-doped[26] and Co-doped samples.[27] However, the high upper critical field is just an estimate of the data based on the single band model with the assumption that the upper critical field is determined by the orbital pair-breaking effect. In the case of multiband superconductivity and paramagnetic limit for the upper critical field, the value of $H_{c2}(0)$ will differ from the value predicted by the WHH theory. Therefore an accurate determination of $H_{c2}(0)$ needs to measure the resistive transitions directly under high magnetic fields. While the high value of $-dH_{c2}/dT$ at T_c at least indicates a rather strong pairing strength with a rather high quasiparticle density of states.

A very interesting point uncovered by our experiment is that the maximum T_c by doping Pt in $BaFe_2As_2$ is 25 K, which is close to that by doping Ni, Co, and Ir at the Fe sites. Manifold interests can be raised here. (1) Although the ionic

sizes are rather different among them, while the maximum T_c is not influenced by them, which may indicate that the non-magnetic centers play a trivial role in the pair-breaking effect. (2) Although the mass of the $5d$ element Pt is much heavier than the mass of the $3d$ elements, such as Ni, again the maximum T_c is the same by doping them to the Fe sites, which trivializes the importance of phonon-mediated mechanism in the occurrence of superconductivity. (3) Normally the $5d$ transition elements have much wider band and stronger spin-orbital coupling effect while the similar maximum T_c may suggest that the electron itinerary as well as the spin-orbital coupling are not the determining factors for the occurrence of superconductivity. Our results here shed lights in the understanding of the mechanism of superconductivity in the iron pnictide superconductors.

IV. CONCLUSIONS

In summary, superconductivity has been found in $BaFe_{2-x}Pt_xAs_2$ with the maximum $T_c = 25$ K. The phase diagram obtained here is quite similar to that by doping Co, Ni, Rh, and Ir to the Fe sites. The resistivity anomaly temperature T_{an} is rather consistent with that of the structure transition. It is found that all samples with doping to the Fe sites showed an very small RRR (below 3), which is much smaller than the value (up to 10) with the out-of-plane dopants, such as K-doped (Ba,Sr)-122. This indicates the doping at Fe sites naturally leads to a strong intrinsic impurity scattering. While surprisingly, superconductivity can still survive up to about 25 K, even with such a strong impurity-scattering effect. The superconductivity is rather robust against the magnetic field with a slope of $-dH_{c2}/dT = 5.4$ T/K near T_c at the doping level $x = 0.1$. Our results clearly indicate that the superconductivity can also be easily induced in $BaFe_2As_2$ by replacing Fe with Pt. This discovery may trivialize the phonon effect, electron itinerancy, and the spin-orbital coupling in the occurrence of superconductivity.

Note added. When preparing this manuscript, we became aware that J. Paglione *et al.* posted a paper concerning the superconductivity in Pt-doped $BaFe_2As_2$.[23] Their results are consistent with ours although they report the result for only one doping level.

*hhwen@aphy.iphy.ac.cn

[1] Y. Kamihara, T. Watanabe, M. Hirano, and H. Hosono, J. Am. Chem. Soc. **130**, 3296 (2008).

[2] X. Zhu, F. Han, P. Cheng, G. Mu, B. Shen, and H. H. Wen, EPL **85**, 17011 (2009).

[3] M. Tegel, S. Johansson, V. Weiss, I. Schellenberg, W. Hermes, R. Poettgen, and D. Johrendt, EPL **84**, 67007 (2008).

[4] M. Rotter, M. Tegel, and D. Johrendt, Phys. Rev. Lett. **101**, 107006 (2008).

[5] K. Sasmal, B. Lv, B. Lorenz, A. M. Guloy, F. Chen, Y. Y. Xue,

and C. W. Chu, Phys. Rev. Lett. **101**, 107007 (2008).

[6] X. C. Wang, Q. Q. Liu, Y. X. Lv, W. B. Gao, L. X. Yang, R. C. Yu, F. Y. Li, and C. Q. Jin, Solid State Commun. **148**, 538 (2008).

[7] D. R. Parker, M. J. Pitcher, P. J. Baker, I. Franke, T. Lancaster, S. J. Blundell, and S. J. Clarke, Chem. Commun. (Cambridge) **2009**, 2189.

[8] F.-C. Hsu, J.-Y. Luo, K.-W. Yeh, T.-K. Chen, T.-W. Huang, P. M. Wu, Y.-C. Lee, Y.-L. Huang, Y.-Y. Chu, D.-C. Yan, and M.-K. Wu, Proc. Natl. Acad. Sci. U.S.A. **105**, 14262 (2008).

[9] X. Zhu, F. Han, G. Mu, B. Zeng, P. Cheng, B. Shen, and H. H. Wen, Phys. Rev. B **79**, 024516 (2009).

[10] H. Ogino, Y. Matsumura, Y. Katsura, K. Ushiyama, S. Horii, K. Kishio, and J. Shimoyama, Supercond. Sci. Technol. **22**, 075008 (2009).

[11] X. Zhu, F. Han, G. Mu, P. Cheng, B. Shen, B. Zeng, and H. H. Wen, Phys. Rev. B **79**, 220512(R) (2009).

[12] N. Ni, M. E. Tillman, J.-Q. Yan, A. Kracher, S. T. Hannahs, S. L. Budko, and P. C. Canfield, Phys. Rev. B **78**, 214515 (2008).

[13] H. Luo, Z. Wang, H. Yang, P. Cheng, X. Zhu, and H. H. Wen, Supercond. Sci. Technol. **21**, 125014 (2008).

[14] A. S. Sefat, R. Jin, M. A. McGuire, B. C. Sales, D. J. Singh, and D. Mandrus, Phys. Rev. Lett. **101**, 117004 (2008).

[15] C. Wang, Y. K. Li, Z. W. Zhu, S. Jiang, X. Lin, Y. K. Luo, S. Chi, L. J. Li, Z. Ren, M. He, H. Chen, Y. T. Wang, Q. Tao, G. H. Cao, and Z. A. Xu, Phys. Rev. B **79**, 054521 (2009).

[16] L. Li, Q. Wang, Y. Luo, H. Chen, Q. Tao, Y. Li, X. Lin, M. He,

Z. Zhu, G. Cao, and Z. Xu, New J. Phys. **11**, 025008 (2009).

[17] S. Sharma, A. Bharathi, S. Chandra, R. Reddy, S. Paulraj, A. Satya, V. Sastry, A. Gupta, and C. Sundar, arXiv:0902.2728 (unpublished).

[18] F. Han, X. Zhu, P. Cheng, G. Mu, Y. Jia, L. Fang, Y. Wang, H. Luo, B. Zeng, B. Shen, L. Shan, C. Ren, and H. H. Wen, Phys. Rev. B **80**, 024506 (2009).

[19] N. Ni, A. Thaler, A. Kracher, J. Q. Yan, S. L. Budko, and P. C. Canfield, Phys. Rev. B **80**, 024511 (2009).

[20] A. C. Larson and R. B. Von Dreele, Los Alamos National Laboratory Report No. LAUR 86–748, 2000 (unpublished).

[21] C. Dong, J. Appl. Crystallogr. **32**, 838 (1999).

[22] P. C. Canfield, S. L. Budko, N. Ni, J. Q. Yan, and A. Kracher, Phys. Rev. B **80**, 060501(R)(2009).

[23] S. R. Saha, T. Drye, K. Kirshenbaum, N. P. Butch, and J. Paglione, J. Phys.: Condens. Matter **22**, 072204 (2010).

[24] L. Fang, H. Luo, P. Cheng, Z. S. Wang, Y. Jia, G. Mu, B. Shen, I. I. Mazin, L. Shan, C. Ren, and H. H.-H. Wen, Phys. Rev. B **80**, 140508(R)(2009).

[25] N. R. Werthamer, E. Helfand, and P. C. Hohenberg, Phys. Rev. **147**, 295 (1966).

[26] Z. S. Wang, H. Q. Luo, C. Ren, and H. H. Wen, Phys. Rev. B **78**, 140501(R) (2008).

[27] Y. J. Jo, J. Jaroszynski, A. Yamamoto, A. Gurevich, S. C. Riggs, G. S. Boebinger, D. Larbalastier, H. H. Wen, N. D. Zhigadlo, S. Katrych, Z. Bukowski, J. Karpinski, R. H. Liu, H. Chen, X. H. Chen, and L. Balicas, Physica C **469**, 566 (2009).